

Wind Tunnel Measurements of the Wake of a Full-Scale UH-60A Rotor in Forward Flight

Alan J. Wadcock
Gloria K. Yamauchi
Edward T. Schairer
NASA Ames Research Center, Moffett Field, CA 94035

Abstract submitted to:
Test & Evaluation Session 69th AHS Annual Forum,
Phoenix, AZ, May 21-23, 2013

Introduction

A full-scale UH-60A rotor was tested in the National Full-Scale Aerodynamics Complex (NFAC) 40- by 80-Foot Wind Tunnel in May 2010 (Ref. 1). The test was designed to acquire a suite of measurements to validate state-of-the-art modeling tools. Measurements include blade airloads (from a single pressure-instrumented blade), blade structural loads (strain gages), rotor performance (rotor balance and torque measurements), blade deformation (stereo-photogrammetry), and rotor wake measurements (Particle Image Velocimetry (PIV) and Retro-reflective Backward Oriented Schlieren (RBOS)). During the test, PIV measurements of flow field velocities were acquired in a stationary cross-flow plane located on the advancing side of the rotor disk at approximately 90 deg rotor azimuth. At each test condition, blade position relative to the measurement plane was varied. The region of interest (ROI) was 4-ft high by 14-ft wide and covered the outer half of the blade radius.

Although PIV measurements were acquired in only one plane, much information can be gleaned by studying the rotor wake trajectory in this plane, especially when such measurements are augmented by blade airloads and RBOS data. This paper will provide a comparison between PIV and RBOS measurements of tip vortex position and vortex filament orientation for multiple rotor test conditions. Blade displacement measurements over the complete rotor disk will also be presented documenting blade-to-blade differences in tip-path-plane and providing additional information for correlation with PIV and RBOS measurements of tip vortex location. In addition, PIV measurements of tip vortex core diameter and strength will be presented. Vortex strength will be compared with measurements of maximum bound circulation on the rotor blade determined from pressure distributions obtained from 235 pressure sensors distributed over 9 radial stations.

Description of UH-60A rotor blade

Figure 1 shows the UH-60A blade planform and the distribution of pressure transducers at each of the 9 radial stations. Particular attention should be paid to the radial location of the trim tab and the inboard edge of the swept tip as these features can often be recognized in the blade wake.

Description of PIV System

The stereo PIV system design was largely driven by constraints imposed by the 40- by 80-Foot Wind Tunnel test section geometry and facility infrastructure. Details of the installation and the challenges working with a large ROI are described in Ref. 2. The primary PIV system comprised two TSI 11 Mp cameras each with a 120mm lens, a Spectra-Physics PIV laser providing ~260 mJ per pulse @ 532 nm wavelength, four MDG seeders emitting 0.75 micron particles, and a large-format (36-in high by 12-in wide) remote-controlled (2 axes) mirror. Figure 2 shows the PIV system installed in the wind tunnel.

The laser and camera systems were synchronized with the rotor so that PIV data were acquired for different rotor blade azimuths relative to the laser light sheet (LLS). A rotary shaft encoder generated a 1/rev trigger pulse as Blade 1, the pressure-instrumented blade, passed aft of the rotor hub. The 1/rev and 4096/rev encoder signals were input to a custom trigger delay box and used to provide fine control over the laser timing. In general, 100 PIV frames were acquired at each test condition.

Results

Table 1 presents a complete list of test conditions for which PIV data were acquired. In Table 1, *delayed azimuth* refers to the position of the primary blade (in this case, the pressure-instrumented blade) relative to the PIV measurement plane. For example, a delayed azimuth of 30 deg corresponds to the primary blade being 30 degrees ahead of the PIV plane as illustrated in Fig. 3. For this paper, multiple rotor test conditions were selected for analysis from Run 73 and Run 83. Run 73 provides a blade sweep through the LLS for $C_T/\sigma = 0.080$ at $\mu = 0.150$ and

uncorrected shaft angle of 0 deg. Run 83 provides a sweep of C_T/σ from 0.070 to 0.120 at $\mu = 0.150$ and uncorrected shaft angle of 0 deg for a single delayed azimuth of 15 deg.

Sample PIV results for a single test condition are shown in Fig. 4. Figure 4(a) shows simple ensemble average in-plane velocity components as vectors scaled with the free stream velocity of 33 m/s. The out-of-plane velocity component is represented by color-coded contours. The trailed wake shows up as the area of reduced velocity drawn in blue. The kinks in the trailed wake are associated with the trim tab for $0.72 < r/R < 0.87$ and the swept tip which has a non-linear pitch distribution outboard of $r/R = 0.93$. Only 25% of available vectors are plotted for clarity. Figure 4(b) shows equivalent out-of-plane average vorticity derived from the simple ensemble average velocity field shown in Fig. 4(a). Noteworthy features include the strong tip vortex from the reference blade 5 deg ahead of the LLS, remnants of the trailed vortex sheet being entrained into the tip vortex, tip vortices from prior blade passages, and a pair of vortices associated with the inboard and outboard edges of the trim tab. The sign of the vorticity associated with the trim tab vortex pair is consistent with the displacement of the trim tab wake above that of the surrounding rotor blade.

Table 1. PIV Test Conditions

NFAC Run No.	Shaft Angle (deg)	M_{tip}	μ	C_T/σ	Delayed Azimuth $\Delta\Psi$ (deg)
73	0	0.650	0.150	0.080	5, 15, 30, 45, 60, 75, 95, 135, 185, 225, 275, 315
75	4	0.650	0.150	0.080	5, 15, 30, 45, 60, 75, 95, 135, 185, 225, 275, 315
78*	-4.82	0.638	0.303	0.087	5, 15, 30, 45, 60, 75, 95
81	0	0.650	0.240	0.070, 0.090	5
81	0	0.650	0.240	0.110	5, 15, 30, 45, 60, 75, 95, 185, 275
83	0	0.650	0.150	0.070, 0.090, 0.110, 0.120	15
83	-6.9	0.650	0.350	0.080	5, 10, 15, 20, 30, 45, 60, 75, 95, 185, 275

* Run 78 matches Flight Counter 8424 from the 1994 flight test program.

Simple ensemble average velocity fields are often of limited value in the determination of vortex properties due to vortex wander, which causes artificial enlargement of the vortex core diameter. In this paper individual *instantaneous* velocity fields will be curve fit in a least squares sense to a planar cut through a model Lamb-Oseen vortex. Averaging the resulting vortex parameters provides both mean and standard deviation values for vortex position, core diameter, strength and orientation. This allows the determination of 95% probability limits for each of the vortex parameters. References 3-5 provide detailed descriptions of the planar curve fit procedure and present vortex parameters deduced from planar curve fits of measured velocity fields to the model Lamb-Oseen vortex. The model used in Ref. 3 assumed a uniform convection speed for the vortex. The current paper will extend the analysis to allow for gradients in the background velocity field. Vortex location and orientation will be compared with equivalent RBOS measurements.

Run 73 provides PIV data acquired for each blade positioned 5 deg ahead of the LLS (delayed azimuths of 5, 95, 185 and 275 deg) for $C_T/\sigma = 0.080$ and $\mu = 0.150$ allowing the direct comparison of vortex location, orientation, core size and vortex strength between the 4 blades. Blade-to-blade differences are also evident in the blade displacement data, showing up as differences in tip path plane. Blade displacement measurements acquired for $C_T/\sigma = 0.080$ at $\mu = 0.150$ will be presented over the full rotor disk for each of the 4 blades, allowing blade tip position at the LLS location to be correlated with PIV measurements of tip vortex position for each of the 4 blades.

Airloads data are available for $C_T/\sigma = 0.060$ to 0.120 at $\mu = 0.150$ and uncorrected shaft angle of 0 deg. Figure 5(a) illustrates the average blade loading, $M^2 C_n$, over the complete rotor disk for $C_T/\sigma = 0.080$ at $\mu = 0.150$ (same rotor test condition as Fig. 4). Attention should be focused on the 2nd quadrant as blade loading determines the strength of the tip vortex that is shed, and any tip vortices shed in the 2nd quadrant will convect downstream and pass

through the vertical plane coincident with the PIV measurement plane. Figure 5(b) shows the radial distribution of blade loading for selected azimuthal locations in the 2nd quadrant. The final paper will show equivalent radial distributions of circulation from which the maximum strength of the trailed tip vortex can be estimated for direct comparison with PIV measurements.

Additional PIV data will be presented from Run 83 for a C_T/σ sweep from 0.070 to 0.120 at $\mu = 0.150$ and uncorrected shaft angle of 0 deg at a single delayed azimuth of 15 deg. PIV data will be used to document tip vortex strength and core diameter as a function of C_T/σ . Airloads data will provide maximum bound circulation as a function of C_T/σ for comparison with PIV values of vortex strength.

Figure 6 shows a typical observation of the rotor wake provided by the RBOS measurement technique at $C_T/\sigma = 0.080$ at $\mu = 0.150$ from Ref. 6. The final paper will provide multiple such observations at each of the rotor test conditions described above. Each population will be averaged to provide mean and standard deviation values for both vortex position and orientation for direct comparison with PIV measurements. Additional information regarding the RBOS technique is provided in Ref. 7.

References

1. Norman, T. R., Shinoda, P. M., Peterson, R. L. and Datta, A., "Full-Scale Wind Tunnel Test of the UH-60A Airloads Rotor," American Helicopter Society 67th Annual Forum, Virginia Beach, VA, May 2011.
2. Wadcock, A. J., Yamauchi, G. K., Solis, E. and Pete, A. E., "PIV Measurements in the Wake of a Full-Scale Rotor in Forward Flight," AIAA paper 2011-370, 29th AIAA Applied Aerodynamics Conference, Honolulu, HI, June 2011.
3. Yamauchi, G. K., Wadcock, A. J., Johnson, W. and Ramasamy, M., "Wind Tunnel Measurements of Full-Scale UH-60A Rotor Tip Vortices," American Helicopter Society 68th Annual Forum, Fort Worth, TX, May 2012.
4. Ramasamy, M., Paetzel, R. and Bhagwat, M. J., "Aperiodicity Correction for Rotor Tip Vortex Measurements," American Helicopter Society 67th Annual Forum, Virginia Beach, VA, May 2011.
5. Bhagwat, M. J. and Ramasamy, M., "Tip Vortex Aperiodicity Correction: Removing Systematic Uncertainty in Core Radius due to Random Uncertainty in Position," 37th European Rotorcraft Forum, Ticino Park, Italy, September 2011.
6. Schairer, E. T., Kushner, L. K., Heineck, J. T. and Walker, L. A., "UH-60 Airloads RBOS Data Report," internal NASA Ames Research Center report, July 2012.
7. Heineck, J. T., Kushner, L. K., Schairer, E. T. and Walker, L. A., "Retro-reflective Background Oriented Schlieren (RBOS) as Applied to Full-Scale UH-60 Blade Tip Vortices," American Helicopter Society Aeromechanics Specialists' Conference, San Francisco, CA, January 2010.

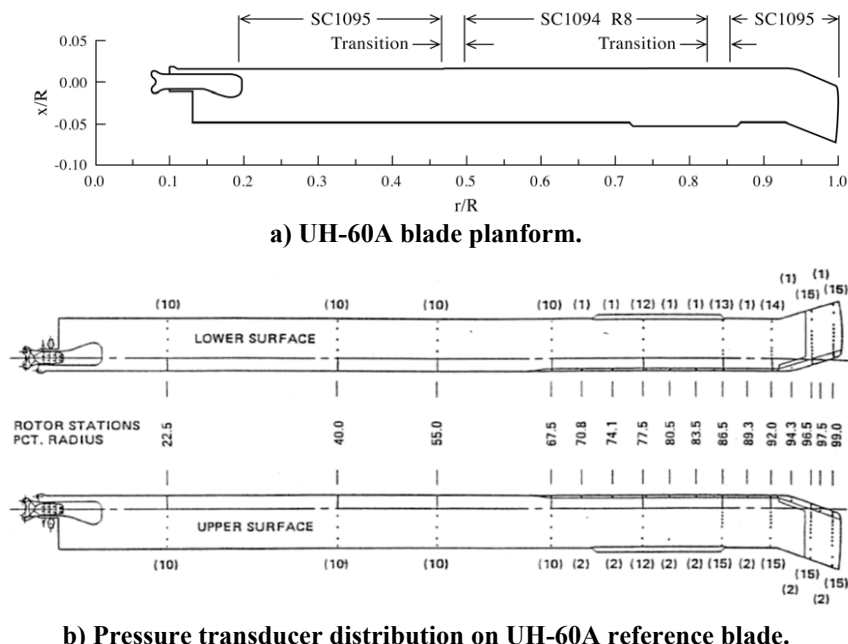


Figure 1. UH-60A blade geometry.

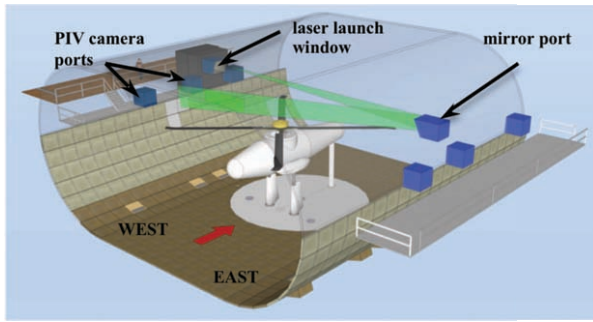


Figure 2. Location of PIV system components in the NFAC 40- x 80-Ft Wind Tunnel.

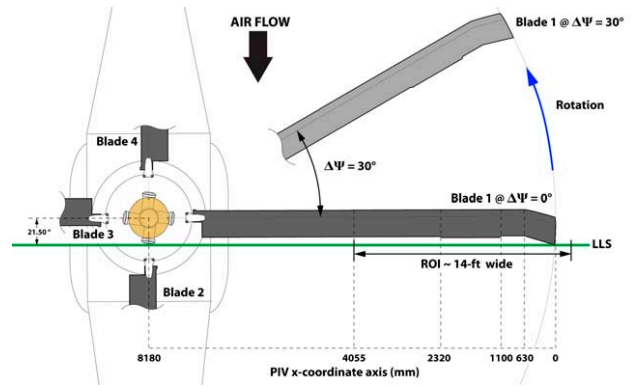
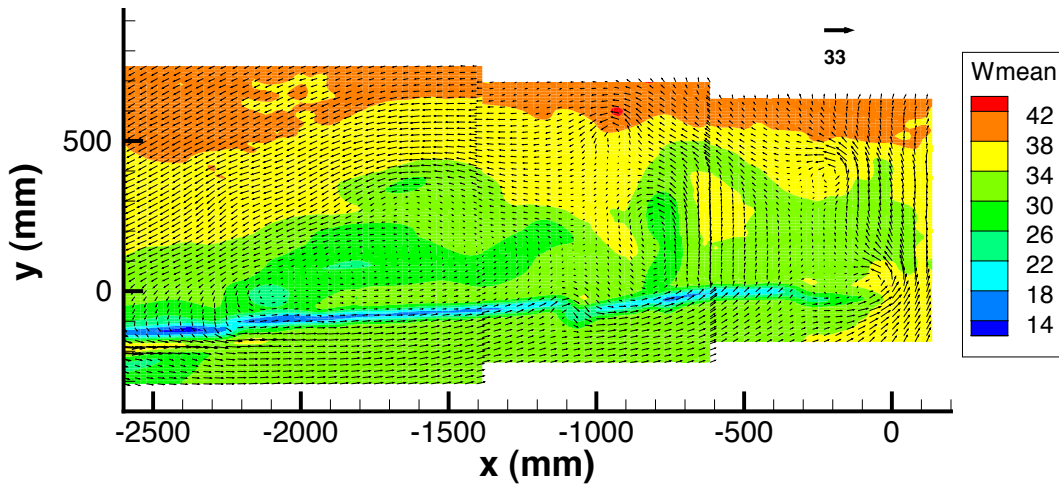
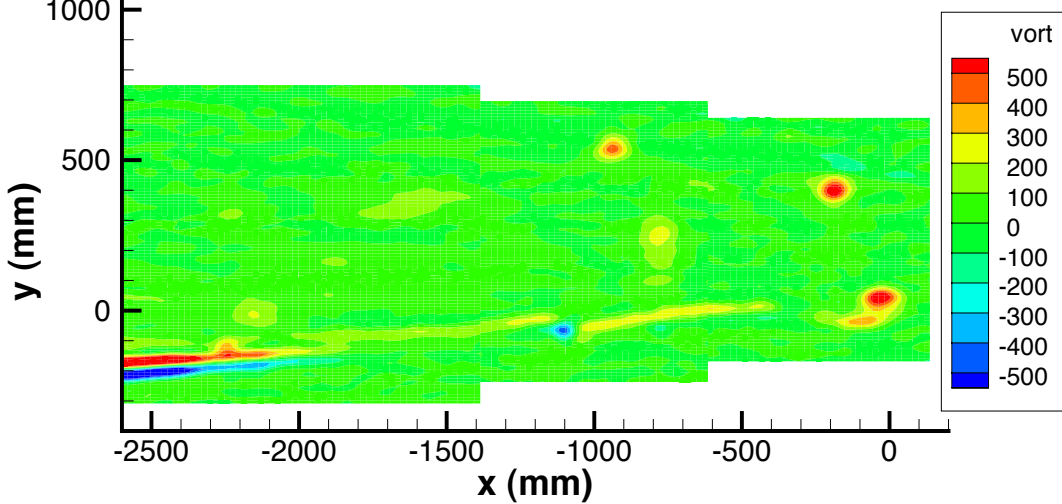


Figure 3. Plan view showing the rotor blade and laser light sheet (LLS) location.

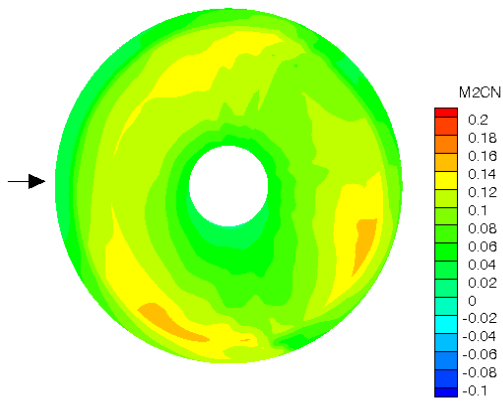


a) Mean velocity field (in-plane velocity vectors, out-of-plane velocity contours).

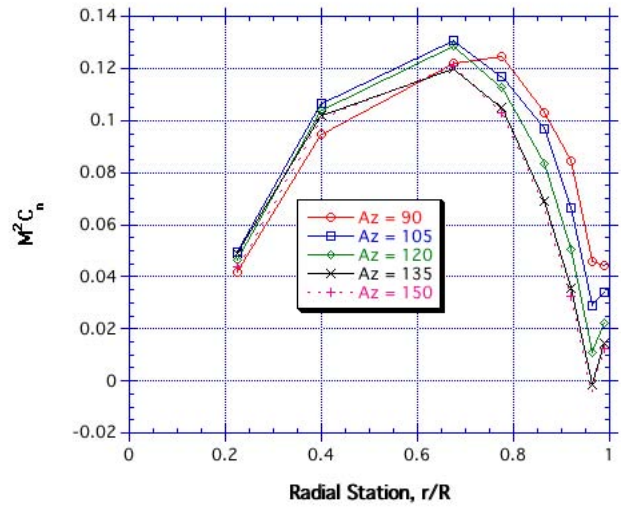


b) Mean vorticity field.

Figure 4. PIV measurement of mean flow field at $C_T/\sigma = 0.080$, $\mu = 0.15$, uncorrected shaft angle = 0 deg; $\Delta\psi = 5$ deg. Ensemble average over outer part of PIV plane; view looking upstream.



a) Average blade loading ($M^2 C_n$) over the complete rotor disk.



b) Average blade loading ($M^2 C_n$) for discrete azimuthal stations in 2nd quadrant.

Figure 5. Average blade loading ($M^2 C_n$) for $C_T/\sigma = 0.080$, $\mu = 0.150$, uncorrected shaft angle = 0 deg.

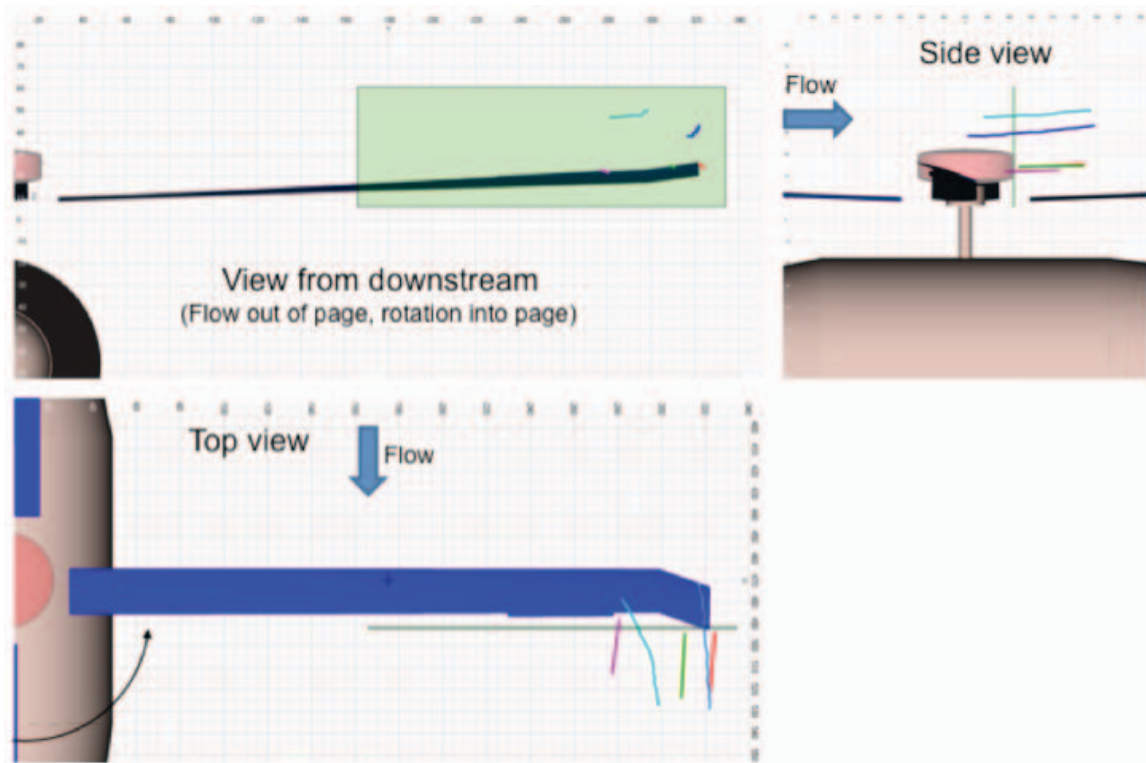


Figure 6. Typical observation of vortex wake provided by single instantaneous RBOS measurement. $C_T/\sigma = 0.080$, $\mu = 0.150$, uncorrected shaft angle = 0 deg; delayed azimuth $\Delta\Psi = 0$ deg.